

Technologist Abstracts

200. SEMI-AUTOMATIC MARKER BASED LOCALIZATION OF THE HEART

Michaela Schmidt,¹ Peter Speier,¹ Okan Ekinci,¹ Jens Guehring,² Edgar Mueller.¹ ¹Siemens Medical Solutions, Erlangen, Germany, ²Siemens Corporate Research, Princeton, NY, USA.

Introduction: Localization of the heart is typically performed using a multi-step approach involving the acquisition of double-oblique slices in order to localize the long and short-axis of the heart. Based on those localizers the standard heart views (2-chamber, 3-chamber, 4-chamber and short-axis views from base to apex) are planned. This approach is operator-dependent, time consuming and requires detailed knowledge of the heart anatomy.

Purpose: We evaluated the feasibility of a marker based approach for localization of the heart which was designed to simplify and speed up the localization procedure. The method developed requires the user to define 4 landmarks on imprecise pseudo short-axis slices acquired with a predefined position and orientation. The standard long axis views including 2-, 3- and 4-chamber views as well as an accurate short-axis view are then automatically calculated and displayed.

Methods: Nine volunteers were imaged on a 1.5 T Siemens MAGNETOM Avanto a Tim system using two six-channel matrix surface coils. All localizers were acquired using a single shot TrueFISP sequence (TR/TE/Flip angle: 2.9ms/1.1ms/70

deg; spatial resolution 2.5 mm × 1.8 mm × 8 mm; acquisition time within cardiac cycle 290 msec) during suspended respiration. The localization process was performed as follows: a) coronal localizer 3 slices. b) Multi-slice localizer (sagittal, coronal, transversal; each 3 slices). Following this step the patient table was moved so that the left ventricle was positioned exactly at the isocenter of the scanner. c) A pseudo (imprecise) short-axis localizer (11 slices) with predefined orientation (transverse to sagittal 43.5 deg. to coronal -28 deg.) and position (left 30 mm; anterior 8 mm; head 10 mm) was acquired without user interaction. d) The user input consisted of setting markers on the centres of the following landmarks: 1. aorta, 2. tricuspid valve, 3. mitral valve, 4. apex based on the pseudo short-axis localizer acquired in step c. With one click in the user interface the 3 standard long-axis views (2-, 3- and 4- chamber view) and one mid-ventricular short-axis (SAX) view were calculated.

Algorithm: The normal vectors (n) of the imaging planes were calculated as follows:

short axis view: $n(\text{SAX}) = \text{normalize}(\langle 3,4 \rangle)$
4 chamber view: $n(4\text{Ch}) = \text{normalize}(\langle 3,2 \rangle \times n(\text{SAX}))$
3 chamber view: $n(3\text{Ch}) = \text{normalize}(\langle 3,1 \rangle \times n(\text{SAX}))$
2 chamber view: $n(2\text{Ch}) = \text{normalize}((n(4\text{Ch}) + n(3\text{Ch}))/2 \times n(\text{SAX}))$

where $\langle a,b \rangle$ is the vector pointing from landmark a to landmark b, and \times stands for the 3-dimensional cross product and $\text{normalize}()$ scales the vector to unit length.

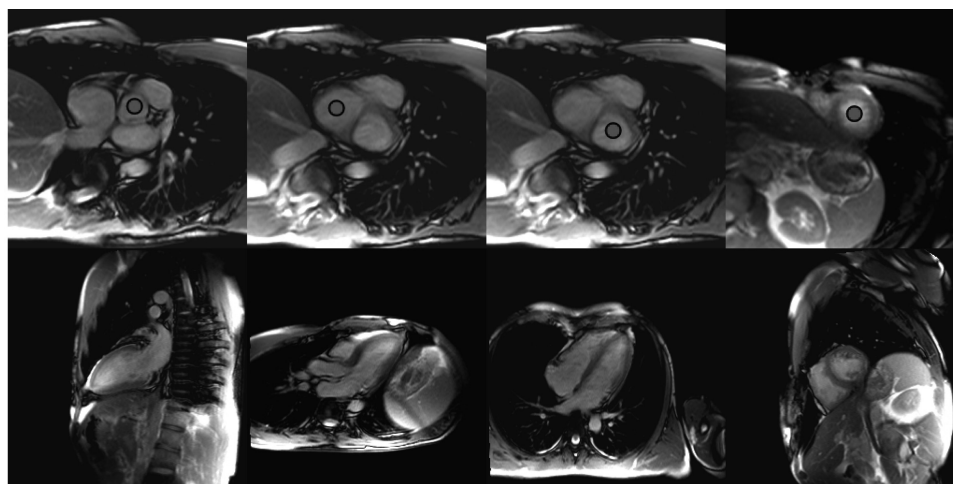


FIG. 1. Pseudo short-axis localizer with marker points (top row) and result images (bottom row).

Results: In all 9 volunteers it was possible to set the landmarks on the standard short-axis localizer. The automatically calculated 36 long- and short- axis views were visually analysed by a cardiologist, experienced with MR and rated on a scale from 1 to 3 (1 = optimal, 2 = minor deviation and 3 = incorrect). 2 (6%) out of 36 segments showed minor deviations; all other views (94%) were rated as optimal. There was no incorrect view.

The mean time from the acquisition of the first localizer to the calculated result images was 3 ± 0.5 minutes.

Representative pseudo short axis images with landmarks and the resulting images are shown in Fig. 1.

Conclusions: We have demonstrated the feasibility of a fast and reliable marker based localization. Further evaluations with patients are ongoing to assess the robustness and the time efficiency of this approach.

201. A COMPREHENSIVE APPROACH WITH MRI IN THE EVALUATION AND VALIDATION OF PAD

John M. Christopher, B.A; RT(R)MR. University of Virginia, Charlottesville, VA, USA.

Purpose: Peripheral Arterial Disease (PAD) is a chronic disease with the atherosclerotic narrowing of the peripheral arteries. The narrowing is a composite buildup of fatty deposits such as lipids and cholesterol, calcium and sometimes thrombus. PAD affects approximately 27 million in North America and Europe and these individuals are also at a higher risk for heart attacks and strokes. At the University of Virginia our CMR research lab has developed a comprehensive imaging protocol which utilizes multiple MR techniques to evaluate and monitor patients with PAD which include high resolution vessel wall imaging, calf muscle perfusion with gadolinium at peak exercise, a bilateral MRA run-off, and phosphocreatine (PCr) recovery time after peak exercise. These techniques were validated by ABI's (ankle-brachial index) at recruitment. This multi-faceted study may improve upon the MR angiography for characterizing disease severity and progression. After the introduction of a statin drug therapy, we will follow up with all these patients to monitor their therapy.

Methods: Patients that were diagnosed with mild to moderate PAD by ABI's were recruited for this study.. Three components of the study, wall imaging for plaque characterization, muscle perfusion after exercise and bi-lateral run-offs are all conducted on a Siemens 1.5T Avanto with current platform and software. A fourth component of the study is where we exercise and evaluate the same calf muscle using P31 spectroscopy. This requires broad-band spectroscopy and is conducted on a Siemens 1.5T Vision-Sonata which is also equipped with the most current platform software. We first assessed the plaque volume by using a custom-built linear four-element ($10 \text{ cm} \times 10 \text{ cm}$ square elements) surface array coil placed over the affected thigh and superficial femoral artery (SFA). A multi-slice turbo-spin-echo

pulse sequence with fat saturation was used. Blood flow was suppressed by using spatial presaturation proximally and distally of the image volume for a black blood technique. Voxel resolution of $0.5 \times 0.5 \times 3 \text{ mm}$ with interleaved image sets used to cover the length of the SFA. A higher resolution tse T1 and T2 were then used for additional plaque characterization. Calf muscle perfusion was evaluated at peak exercise using first pass contrast enhanced imaging immediately following exercise on a custom built ergometer. A modified spoiled gradient echo pulse sequence was employed to accommodate the simultaneous acquisition of muscle perfusion in a distal imaging plane and the arterial input function (AIF) in a proximal plane. We began the imaging at infusion using 100 measurements. Inversion-recovery (TI = 320 ms) was used for muscle imaging and saturation-recovery (TI = 10 ms) was used to image the AIF. Standard MR gadolinium-DTPA enhanced angiography from the abdominal aorta to the foot was performed with a moving table/bolus chase technique in 3 stations and biphasic. Phosphocreatine recovery (PCr) time was analyzed by 31phosphorous (31P) spectroscopy during recovery from peak exercise. 31P spectra were acquired using a single-pulse, surface coil localized, 512 ms free induction decay acquisition with the coil centered on the mid-calf. A standard 31P surface coil was employed. Siemens spectroscopy software was used to estimate relative concentrations of adenosine triphosphate (ATP), PCr and Pi. PCr recovery time was then calculated.

Results: There's a strong correlation of data between these multiple techniques and the findings with ABI and angiography.

Conclusions: We have shown the usefulness of a comprehensive approach to evaluating PAD. Plaque volume in the SFA wall correlates well with both calf muscle perfusion and MRA findings. These techniques used together have the potential to improve the ability to characterize and risk stratify PAD patients, as well as monitor disease progression and response to novel therapies.

202. IMAGE RECONSTRUCTION FROM RANDOMLY UNDERSAMPLED DYNAMIC MRI DATA

Urs Gamper, Peter Boesiger, Sebastian Kozerke. Institute for biomedical engineering, Zurich, Switzerland.

Introduction: Dynamic images of typical objects in MRI are highly redundant in space and time. Methods have been proposed that exploit this spatiotemporal correlation to allow speeding up the data acquisition process by undersampling on a regular grid in $k-t$ space (1). With $k-t$ BLAST temporal blurring is introduced due to partial volume effects in the training data. At low reduction factors this blurring is subtle but can become noticeable (Fig. 1). Recently, a method was proposed that allows an *exact* image reconstruction from randomly undersampled Fourier samples (2) by minimizing the L^1 -norm of the image in a sparse domain. Since the Fourier transform along the temporal dimension ($x-f$ space) provides a sparse representation of the data this method can straightforwardly be used and a

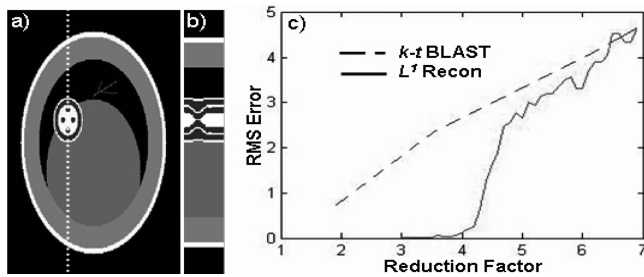


FIG. 1. A test dataset (a) was used. The temporal evolution along the dotted line is shown in (b). The total reconstruction errors for this $x-t$ dataset are shown in (c). Below a certain reduction factor (depending on the sparsity of the data) the L^1 reconstruction results in an exact replica of the fully sampled data.

further sparsifying transform such as the wavelet transform (3) is not needed.

Methods: Data were acquired on a 1.5T Philips Achieva whole body MR system (Philips Medical Systems, Best, NL) using a 5-element coil array. A balanced SSFP sequence with high temporal resolution for resolving the dynamics of valvular leaflets was used with the following parameters: spatial resolution = $1.6 \times 1.6 \times 8 \text{ mm}^3$, TR = 3.4 ms, $\alpha = 60^\circ$, cardiac phases = 78. The k -space was randomly undersampled along the phase encoding and temporal dimension by a factor of 3 resulting in a total scan duration of about 17s allowing for single breath hold acquisitions. With $k-t$ BLAST, a $k-t$ factor of 4 was used which corresponds to a net acceleration factor of 3.36. The reconstruction of the randomly undersampled data was done off-line in MATLAB. Although a convex L^1 minimization problem is mathematically tractable it is computationally demanding due to the large number of free variables. Therefore a simple steepest descent algorithm along the energy difference between the reconstructed and the measured $x-f$ space was used. Due to the properties of the point-spread function of a random sampling scheme this results in a minimal L^0 norm of the $x-f$ space which features the same properties as the L^1 norm.

Results: Figure 1 shows simulation results based on a model data set. It is seen that results from randomly undersampled data yield an exact reconstruction of the object for small reduction factors. Fig. 2 compares in-vivo results acquired with

$k-t$ and random undersampling. As expected, the random undersampling scheme preserved image sharpness along the temporal dimension.

Discussion: Nonlinear reconstruction methods for undersampled data feature interesting properties. Up to a certain acceleration factor (depending on the sparsity of the data) this reconstruction is exact, resulting in an increased image quality and temporal fidelity compared to e.g. the $k-t$ BLAST reconstruction method. Higher acceleration factors result in similar reconstruction RMS errors for both methods although the trait of the artifacts is different. The L^1 reconstruction features noise-like artifacts which might be less disturbing to the observer's eye than ghosting or temporal filtering. Altogether the L^1 reconstruction is well suited for dynamic imaging and can complement other acceleration techniques.

REFERENCES

1. Tsao J. et al. Magn Reson Med 2003;50(5):1031–1042.
2. Candes E et al. Robust uncertainty principles: Exact signal reconstruction from highly incomplete frequency information. 2005.
3. Lustig M. et al. Proc Intl Soc Mag Reson Med 2006;14(2420).

203. ASSESSMENT OF VENTRICULAR FUNCTION IN PEDIATRIC PATIENTS USING RAPID ACQUISITION MULTI-SLICE TRUEFISP IMAGING AND TSENSE, WITH AND WITHOUT BREATH-HOLD

Glenn D. Cahoon, Master of Applied Science,¹ Michael Ditchfield, MD FRANZCR,¹ Michael Cheung, MD,¹ Wellesley Were, BAppSc.² ¹Royal Children's Hospital Melbourne, Parkville, Australia, ²Siemens Medical Systems, Sydney, Australia.

Introduction: Cardiac Magnetic Resonance (CMR) has become widely accepted as the 'gold standard' technique for the evaluation of ventricular function (Fieno et al., 2006). CMR is particularly useful in the pediatric population, given that other available techniques are either less reliable, more invasive or have an increased requirement for sedation or anaesthetic. The application

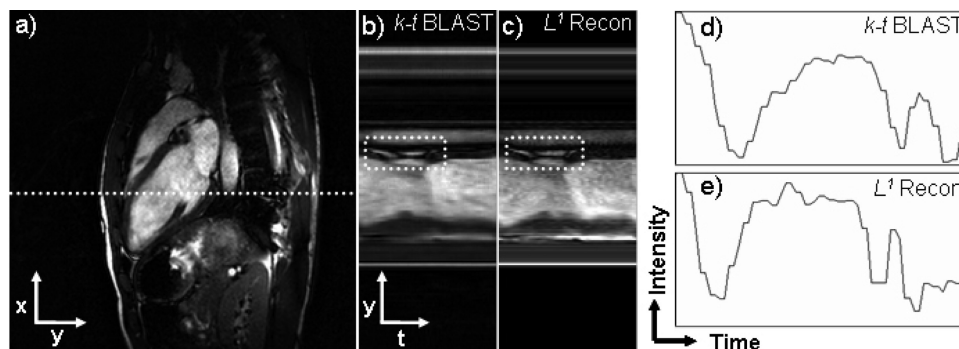


FIG. 2. (a) First frame of long axis cine acquisition. The temporal evolution along the dotted line in (a) is shown for the different reconstruction methods in (b) and (c). Intensity profiles along the Central line in the dotted squares in (b) and (c) are shown in (d) and (e). The increased temporal fidelity of the L^1 reconstruction is shown by the smaller transition widths in (e).

of CMR is complicated in pediatric settings, however, due to reduced comprehension and compliance with instructions among children, such as those involving reproducible breath-hold techniques. New parallel imaging techniques allow us to dramatically accelerate imaging sequences, by reducing the number of phase encoding lines acquired. Unfortunately, pediatric patients are already at the limit of spatial/temporal resolution, due to smaller anatomical structures and increased heart rate, thus limiting the effectiveness of these techniques in clinical practice. An alternative approach that may offer a significant advantage over available techniques is adaptive sensitivity encoding incorporating temporal filtering (TSENSE). This technique may provide the opportunity to accurately assess ventricular function within a dramatically decreased time frame. While data are available in the adult setting, no previous research has evaluated the use of TSENSE in assessing ventricular function within a pediatric patient population.

Purpose: The aim of this study was to investigate the effect of spatial and temporal resolution in accurately assessing ventricular function, and to determine the optimal imaging parameters for the TSENSE sequence in a pediatric patient sample. The accuracy of the TSENSE technique was determined at varying resolutions and number of cardiac phases, when compared to our standard multi-slice, multi-breath-hold True FISP technique (MS-MBT).

Methods: Data were collected from 12 pediatric patients. Scans were acquired on a Siemens Avanto 1.5T MRI system. In each patient a short axis stack (SAX) was obtained through the entire volume of the left ventricle (280-320FOV, 10-15 slices, 5-7 mm, no gap) using MS-MBT. The SAX was repeated using single breath-hold TSENSE with the same parameters, and again using free breathing TSENSE at three different resolutions (192, 160, 128 matrix). The volumetric data were analysed and the End Diastolic Volume (EDV), End Systolic Volume (ESV), Stroke Volume (SV) and Left Ventricular Mass (LVM) determined. Data were analysed using partial correlation, controlling for test-retest and inter-rater reliability estimates.

Results: Controlling for reliability indices, positive correlations of volume ratings using the TSENSE and MS-MBT were obtained for all sequence types ($p < .001$). There was no significant difference between single breath-hold TSENSE and free-breathing TSENSE ($r = .95$, $r = .92$, respectively). Estimates of LVM using TSENSE more closely approached ratings of LVM using MS-MBT at higher spatial resolutions ($p < .05$). In contrast, spatial resolution was unrelated to the estimates of ventricular volumes. The number of cardiac phases acquired was affected by patient heart rate and the imaging parameters of the TSENSE sequence. Careful selection of the imaging parameters resulted in a TSENSE sequence that was sensitive to both ventricular volumes and LVM estimations.

Conclusions: This study demonstrated that the TSENSE technique could be adapted to evaluate ventricular function in a pediatric patient sample. While high-resolution multi-breath-hold TrueFISP CINE imaging remains the technique of choice for the

assessment of ventricular function, adaptive TSENSE will yield reliable results within a shortened scan time among children who are unable to comply with standard breath-hold imaging techniques. Optimal imaging parameters for pediatric CMR based on our findings will be presented. Further research is required to confirm these findings and further refine optimal sequences for use in the pediatric setting.

204. METHOD TO DETERMINE A COMPLETE CARDIAC T_1 MAP WITHIN A SINGLE BREATH-HOLD

J. B. M. Warntjes,¹ J. Kihlberg,¹ J. Engvall.² ¹Center for Medical Imaging and Visualisation, Linköping, Sweden, ²Division of Clinical Physiology, Linköping, Sweden.

Introduction: Cardiac viability is in clinical practice measured with the so-called late enhancement method (1). A T_1 contrast agent is administered and after a time of about 10 mins an inversion recovery image is taken of the heart. A difference in contrast can be seen between ischemic and healthy tissue owing to the different contrast uptake. To maximize contrast the inversion time is set such that the healthy tissue appears black. Finding the optimal inversion time takes valuable clinical time and is demanding for the patient. An improvement was the phase sensitive method (2) where the phase information in the images is taken to correct for the sign of the modulus values. The sign-corrected images can be windowed such that the healthy myocardium appears black.

Method: In the proposed method a quantitative T_1 map is measured for the whole cardiac volume within one breath-hold. This is done by means of two stacks of images, one with inversion pulses at a certain inversion time and one stack without. The k-spacing filling is done with a low-high profile order such that both image intensities are proportional with the unsaturated magnetization M_0 . A single heart beat waiting time is put between the measurements to ensure an unsaturated state to start the second measurement. The latter stack of image is directly proportional to the proton density (disregarding T_2^* and flip angle inhomogeneity effects). Using both stacks T_1 can directly be calculated. With the known proton density and T_1 relaxation time the contrast image at any desired inversion time can be calculated in post-processing. In the figure an example is demonstrated of a short-axis slice of a patient with ischemia. In the left panel the T_1 map is shown, in the center panel the calculated late enhancement image, where the inversion time was chosen such that myocardium appears black and in the right panel the actual late enhancement image is shown. In the quantification scan 12 slices were measured with a 192^2 matrix within 19 heart beats, corresponding to a scan time of 15-20 s. In order to achieve this high speed a 3D TFEPI sequence was used with EPI factor 5 and Sense factor 2.

Outlook: The method can be extended by taking a third stack of images with a high-low profile order. Instead of M_0 these images are proportional to the saturated magnetization M_0^* . The

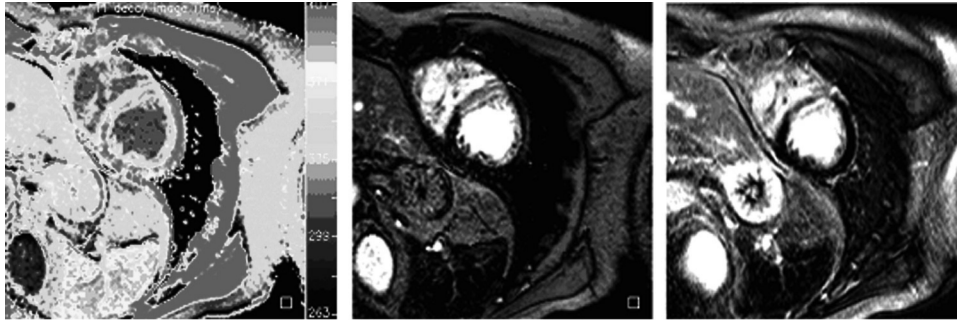


FIG. 1.

intensity of the saturated images depends on T_1 and the actual local flip angle. Since T_1 is already known from the first two stacks of images the local flip angle, or the B_1 inhomogeneity, can be calculated. This will improve the estimation of proton density and therefore the late enhancement image.

Other clinical areas where this method may be useful include T_1 estimation for the assessment of fatty livers, quantification and classification of atherosclerotic plaques, fast T_1 estimation in the brain for diseases such as Alzheimer and Multiple Sclerosis and determination of water concentration of oedema in the brain.

REFERENCES

1. Wendland MF, Saeed M, Lund G, Higgins CB. Contrast-enhanced MRI for quantification of myocardial viability. *J Magn Reson Imaging* 1999;10:694–702.
2. Kellman P, Arai AE, McVeigh ER, Aletras AH. Phase-sensitive inversion recovery for detecting myocardial infarction using gadolinium-delayed hyperenhancement. *Magn Reson Med* 2002;47:372–383

205. A SELF GATED FREE BREATHING APPROACH FOR CARDIAC IMAGING

Martin Buehrer, Peter Boesiger, Sebastian Kozerke. ETH Zürich, Zürich, Switzerland.

Introduction: Free breathing cardiac acquisition generally requires the use of an electrocardiogram (ECG) and a respiratory navigator placed on the diaphragm. Both these techniques are prone to errors and increase the complexity of cardiac imaging. The ECG is susceptible to RF interference and the navigator signal might not fully reflect the respiratory motion on the heart. In this work a self gated, triggered, free breathing approach is presented which requires neither ECG gating nor respiratory navigation.

Methods: In previous work a modified SSFP sequence was presented which provides a signal synchronous to cardiac motion by additionally sampling a few points in the k-space center after every read out train (1). This signal was then used for cardiac triggering. In this work the approach is extended to free breathing. Using the same sequence in combination with free breathing provides a signal composed of respiratory and cardiac

synchronous variations (Fig. 1a). Since both cycles usually have different and well defined frequencies the superimposed signals can be separated and used for respiratory gating and cardiac triggering. For this purpose a wavelet filter was applied to the raw signal.

To test the feasibility of the approach a 2D cine short axis view of the heart was acquired (TR = 4.5 ms, TE = 1.8 ms, flip angle = 60° , scan matrix = 192×187 , FOV = 320×273 mm²). Groups of 8 k-space lines were repeatedly acquired over a period of approximately 9s to cover the whole respiratory cycle. For obtaining the motion signal 20 additional points in the k-space center were sampled and averaged. For reference signals from an ECG and respiratory belt were simultaneously acquired. Using the respiratory and cardiac synchronous signal the acquired data were prospectively reconstructed to a triggered

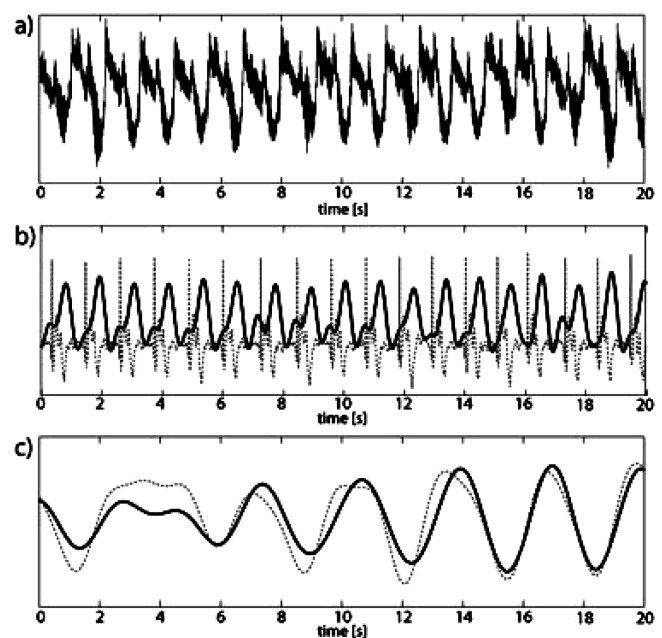


FIG. 1. The motion dependent singles used for triggering and gating. a) the raw single obtained by averaging the k-space center. b) the wavelet filtered cardiac synchronous single and a simultaneously acquired ECG for reference (dotted line) c) the wavelet filtered respiratory synchronous single and the single from a respiratory belt as reference (dotted line)

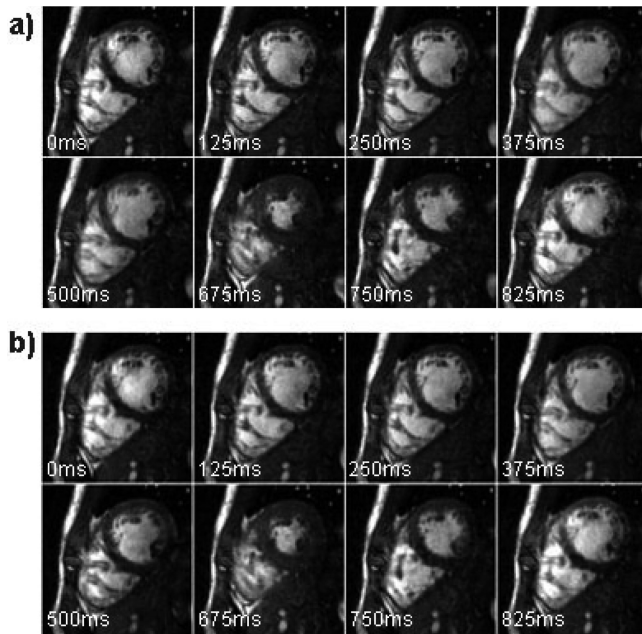


FIG. 2. Reconstructed self gated images from a 2D cine short axis view without use of ECG or respiratory gating. Eight out of 30 heart phases are shown reconstructed on an acquisition window of 30 ms per heart phase. Profiles corresponding to a gating level lower than 20% of the maximum value were rejected (b). For comparison the same dataset is shown but reconstructed using data from a simultaneously acquired ECG and respiratory belt for cardiac triggering and respiratory gating.

cine scan with an acquisition window of 30 ms per heart cycle. Data corresponding to a gating level lower than 20% of the maximum value were rejected.

Result: As seen in Fig. 1 the superimposed raw signal can be nicely separated into a respiratory and cardiac synchronous signal with good correspondence to the ECG and respiratory belt. Using this information for respiratory gated and cardiac triggered images free of motion artifacts can be reconstructed (Fig. 2).

Discussion: Preliminary experiments have shown that the signal obtained from the center k-space can be used for cardiac triggering and respiratory gating. Doing so cardiac images can be reconstructed without using any additional technique such as ECG or respiratory navigator. Also gating and triggering is performed on a signal obtained directly from the anatomy of the heart.

REFERENCE

1. Crow M.E. et al., MRM 2004;52:782–788.

206. BRIGHT IS NOT ALWAYS DEAD—A CASE STUDY ON IR-GE IMAGES

Robin Nijveldt, MD, Aernout M. Beek, MD, Tjeerd Gernans, MD, Marco J. W. Goette, MD, PhD, Mark B. M. Hofman, PhD, Albert C. van Rossum, MD, PhD. *VU University Medical Center, Amsterdam, The Netherlands.*

Introduction: Myocardial infarction (MI) can be detected with high accuracy using late gadolinium-enhanced CMR, where a high concentration of contrast in areas of MI causes high signal intensity on inversion recovery-gradient echo (IR-GE) images, leading to the aphorism “bright is dead”. However, it is not clear whether high signal intensity in myocardium on IR-GE is solely caused by contrast enhancement or by other mechanisms as well, and whether IR-GE images can identify other tissue characteristics than areas of an expanded extracellular matrix alone.

Purpose: To evaluate the potential of tissue characterization of IR-GE imaging in patients with ischemic and non-ischemic heart disease, and compare it with conventional techniques.

Methods: In 6 patients (3 ischemic, 3 non-ischemic) with a hypo-intense area in the myocardium on cine imaging, T1-weighted turbo spin echo (TSE) images and IR-GE images without contrast were acquired. In areas with high signal intensity and in remote non-enhanced myocardium, SNR and CNR were measured on T1-weighted TSE and IR-GE images. In 5 patients, additional late gadolinium-enhanced IR-GE imaging was performed, 15 minutes after administration of 0.2 mmol/kg Gd-DTPA. Inversion time was optimized to null the signal of remote myocardium in all IR-GE images.

Results: In all patients, the hypo-intense area on cine imaging appeared as an area of high signal intensity on IR-GE images before administration of contrast (A), and was confirmed to be adipose tissue on T1-weighted TSE images (B, white arrow heads). The hyperenhanced area was clearly visible on both techniques, and although SNR was higher on T1-weighted TSE images (88.8 ± 50.4 vs 30.0 ± 7.8 , $p < 0.01$), CNR was comparable (36.2 ± 29.6 vs 23.1 ± 7.5 , $p = 0.33$). The hyperenhanced area was surrounded by areas of myocardial fibrosis on late gadolinium-enhanced IR-GE images in all ischemic patients

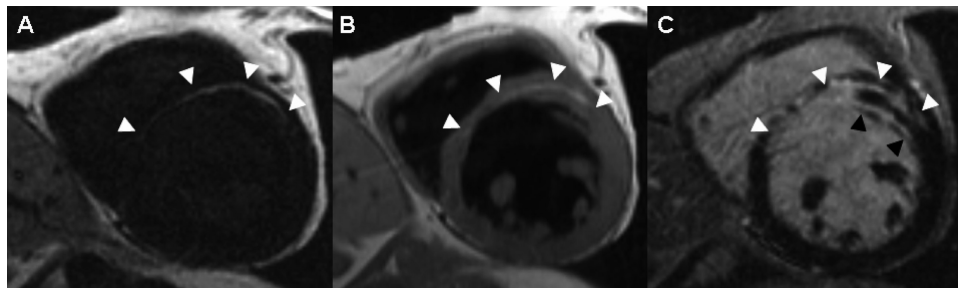


FIG. 1.

(C), consistent with lipomatous metaplasia. The hyperenhanced area of 2 non-ischemic patients was still visible on late contrast-enhanced IR-GE images.

Conclusions: This case study demonstrates that not only contrast in an expanded extracellular matrix has the privilege to increase signal intensity on IR-GE images, and that IR-GE imaging can be used to identify areas of adipose tissue with comparable CNR as T1-weighted TSE imaging.

207. THE UTILISATION OF NEW CMR TECHNIQUES WITH A PEDIATRIC POPULATION: CASE STUDIES FROM THE ROYAL CHILDREN'S HOSPITAL, MELBOURNE

Glenn D. Cahoon, Master of Applied Science,¹ Michael Ditchfield, MD FRANZCR,¹ Michael Cheung, MD,¹ Michael Kean¹, Wellesley Were, BAppSc.² ¹Royal Children's Hospital Melbourne, Parkville, Australia, ²Siemens Medical Systems, Sydney, Australia.

Cardiac magnetic resonance (CMR) represents an ideal technology for the diagnosis and management of pediatric cardiac conditions. Advantages include the ability to image in any plane, accurately quantify blood flow, and conduct functional imaging, without the use of ionizing radiation. These advantages are particularly helpful in delineating the complex congenital abnormalities often found in pediatric conditions. There exist, however, a number of technical challenges with standard CMR techniques that result from smaller anatomical structures, faster heart rates, and poor patient compliance. Recent advances in MRI hardware and sequence design allow us to overcome many of these limitations of spatial and temporal resolution traditionally inherent in pediatric CMR, while dramatically reducing overall scan time. These new advances offer exciting opportunities to greatly increase the utility of CMR with pediatric patient populations.

This presentation is a review of our experience in using these new technologies in pediatric CMR at both 1.5T and 3T over the past year. The author will describe and present a series of case studies, demonstrating the use of new CMR techniques. These techniques include recent 'works in progress', such as T2 prepared TrueFISP imaging, 3D whole heart morphological studies, time resolved contrast enhanced MRA, phase contrast flow quantification with iPAT (GRAPPA), and dynamic cardiac imaging with TSENSE. This presentation will also describe the fundamentals of CMR pulse sequences, and the integration of these new techniques into our current protocols. In addition, differences in imaging strategies and patient preparation for pediatric CMR will be discussed. The cases, selected from patients referred for CMR at the Royal Children's Hospital, Melbourne, represent a mix of congenital and acquired cardiovascular diseases over a range of age groups from neonatal to adolescent and early adult presentations. All the images were acquired

using either our 32 Channel TIM Avanto 1.5T, or TIM TRIO MRI systems. This presentation demonstrates the utility of new advances in CMR to dramatically improve patient diagnostics across a range of pediatric cardiac conditions.

208. EVALUATION OF SINGLE-SHOT SSFP TECHNIQUE FOR ASSESSING MYOCARDIAL VIABILITY

Mercedes Pereyra, RT,¹ David Rammage, RT,¹ Steffen Huber, MD,¹ Debra Dees, RN,¹ Brenda Lambert, RN,¹ Benjamin Cheong, MD,¹ Scott D. Flamm, MD,¹ Raja Muthupillai.² ¹St. Luke's Episcopal Hospital, Houston, TX, USA, ²Philips Medical Systems and Baylor College of Medicine, Houston, TX, USA.

Introduction: A recently described MR imaging method, delayed enhancement (DE) imaging, has been shown to be capable of identifying regions of irreversible myocardial injury with exquisite spatial and contrast resolution (1, 2). Therefore, DE MRI can play a vital clinical role in aiding the management of patients with acute and/or chronic coronary artery disease.

Conventional 2D-DE MRI techniques acquire a single slice per breath hold, with each breath-hold lasting about 8–16 seconds long. Thus an entire evaluation of the left ventricle (LV) requires several breath-holds. However, the 2D-DE MRI technique is not only time consuming but is also not suitable for many groups of patients, e.g., those who can not sustain a consistent reproducible breath-hold, patients with severe arrhythmias etc.

Purpose: The purpose of this study is to evaluate the role for a single shot SSFP imaging in the assessment of myocardial viability by direct comparison with conventional 2D DE-MRI technique using quantitative metrics.

Materials and Methods: Subjects: 10 patients (9M, age: 52 ± 12 yrs) referred for MR viability assessment were included in the study. Six subjects had irreversible myocardial injury. All subjects gave written informed consent.

Data acquisition: A cardiac gated inversion recovery prepared segmented gradient echo technique was used for data collection. The conventional two-dimensional viability (2d-Viab) sequence acquired data every other heart-beat using a T₁ weighted gradient echo readout. The single shot imaging technique used a SSFP readout (2D-SSh). Other acquisition parameters for the two techniques are shown in Table 1. A series of 10-12 contiguous slices were obtained using both the techniques to cover the entire left ventricle (LV).

Quantitative Analysis: All images were transported to a workstation (View Forum, software release level 5.x. Philips Medical Systems) for further processing and detailed analysis. Regions-of-interest were drawn on the images obtained using the 2D-Viab, and 2D-SSh techniques to compute the myocardial signal-to-noise ratio (SNR_{myo}), and infarct-to myocardial contrast-to-noise ratio (CNR_{inf_mus}). In addition, the scar burden was quantified for each patient using a thresholding approach.

TABLE 1
MR acquisition parameters and Results

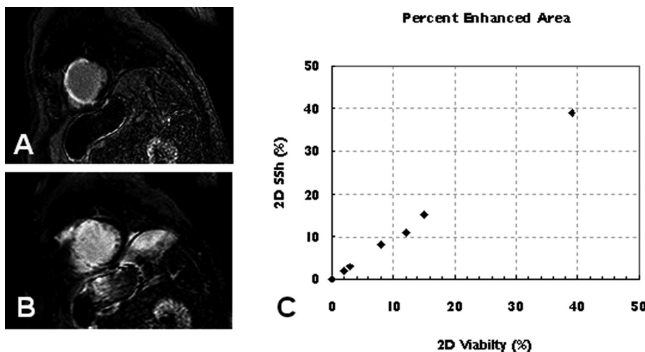
Parameter	2d-Viability	2d-SSh-SSFP
Type of Readout	T ₁ -TFE	SSFP
Act TR/TE (ms)	4.3/2.1	2.7/1.37
Acquired Voxel size (mm)	2/2.4/10	2/2.5/10 mm
TFE Factor	32	50
TFE acquisition duration (ms)	137.7	137.1
Scan time (s)	9	1
Quantitative ROI Analysis Results		
SNR _{myo}	3.4 ± 1.6	1.7 ± 1.6
CNR _{inf-myocardium}	18 ± 5.8	21.4 ± 10.3

The endo-cardial and epi-cardial contours were drawn on the delayed enhancement images by an experienced observer. The pixels with signal intensities (SI) that were at least 2 standard deviations (SD) greater than the mean SI of the normal remote myocardium were classified as scar.

Statistical Analysis: All data are presented as mean ± standard deviation (SD). A p value of less than 0.05 was considered significant. Pair wise t-tests were used to compare differences between means of two groups.

Results: All patients were successfully imaged using both techniques (Figure 1). The results from the SNR and CNR analysis are listed in Table 1. The low myocardial SNR for both techniques reveals that it is possible to effectively suppress the signal from normal remote myocardium. The 2D SSh approach had a slightly greater infarct-to-myocardial CNR, and this difference was statistically significant ($p < 0.05$). The percent of pixels that showed enhancement were virtually similar for both techniques, and there was no statistically significant difference between the two techniques.

Conclusions: The results from this study show that a single shot viability imaging with a SSFP readout provides quantitative information that is comparable to that provided by the conventional 2D viability imaging technique. In addition, the percent of pixels classified as scar were virtually identical for both techniques, despite the slightly lower spatial resolution of the 2D SSh-SSFP technique.



REFERENCES

1. Simonetti OP, Kim RJ, Fierno DS, et al. Radiology 2001;218:215–23.
2. Kim RJ, Fierno DS, Parrish TB, et al. Circulation 1999;100:1922–2002.

209. FINITE ELEMENT ANALYSIS OF LEFT VENTRICULAR CONTRACTILITY USING MR VELOCITY MAPPING

Su-Lin Lee,¹ Andrew Huntbatch,¹ David Firmin,² Guang-Zhong Yang,¹ ¹Imperial College London, London, United Kingdom, ²Royal Brompton and Harefield Trust CMR Unit, London, United Kingdom.

Introduction: With the increasing versatility of CMR, a natural step towards the further understanding of intrinsic myocardial contractility is to perform subject-specific biomechanical modelling by effectively integrating the structural and functional information available. The purpose of this study is to describe a finite element modelling scheme based on myocardial velocity imaging where subject-specific velocity information is used to control the finite element simulation.

Methods: Short-axis velocity mapping images of the heart were acquired from three normal male subjects using a gradient-echo phase-contrast protocol (TR = 53 ms, TE = 7.1 ms, in-plane pixel resolution = 1.17 × 1.17mm, FOV = 30 × 30 cm, VENC = -15 to +15 cm/s) on a 1.5T Siemens Sonata MRI scanner. The sequence consisted of specially designed black-blood RF pulse being applied every other time frame followed by the imaging pulse. A total of 12 to 14 short axis slices were obtained for each subject with 13 to 17 timeframes spanning the entire cardiac cycle. The epicardial and endocardial borders of the left ventricle (LV) were segmented from the magnitude images and were used to build a volumetric model of hexahedral elements. To generate elements of sufficient size, the elements were divided using subdivision solids (1) (Figure 1).

An anisotropic elastic material model was applied to the elements, mimicking the nonlinear properties of the cardiac fibres. A fibre direction is defined at each element and at the epicardial border are taken to be -60° and at the endocardial border, 60° (2). As the velocity information is available across a set of images spanning different phases of the cardiac cycle, each timeframe is simulated separately. The intra-ventricular pressure change applied follows the *a priori* pressure distribution of the LV deforming through systole to diastole. ANSYS (ANSYS,

TABLE 1
Mean error of the x, y and z components of the strain rates at a basal region at maximal systole and diastole of the simulations.

Timeframe	Strain Rate Error (s ⁻¹)		
	x	y	z
Systole	-0.00553 ± 0.012	0.00136 ± 0.0025	-0.0585 ± 0.18
Diastole	0.0312 ± 0.024	-0.0383 ± 0.032	0.0410 ± 0.032

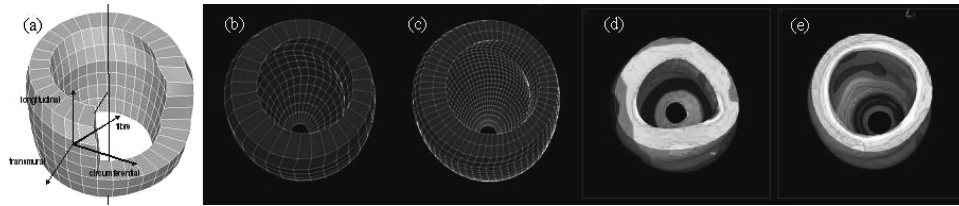


FIG. 1. (a) The fibre directions. (b-c) A volumetric model of the LV and the subdivided model with subdivision. Deformation and Von Mises stress of the LV from one subject studied at maximal systole (d) and diastole (e).

Inc., Cannonsburg, PA) was used for the optimisation of the deformation.

Results: A reconstructed LV is presented at maximal systole and diastole, along with the Von Mises stress, in Fig. 1. The deformation is as expected - when at systole, the LV contracts and shortens and there is evidence of radial twisting. Table 1 illustrates the errors of the x , y , and z components of the strain rates at the basal regions of the LVs between the real data and the reconstructed technique. It is evident that the residual error is relative small, suggesting the quality of the optimisation process.

Conclusion: We have presented a finite element modeling scheme based on myocardial velocity imaging where subject-specific velocity information is used as a boundary condition. The results presented show deformation of the LV that corresponds to the movement expected in a normal heart. Strain distribution graphs also show results as expected, with circumferential strain negative during systole (shortening) and positive during diastole (lengthening) and radial strain the opposite (corresponding to wall thickening). The technique fits well to the strain rates from the original MR velocity data, suggesting the internal consistency of the algorithm. The technique requires little user interaction and provides good initial results with a relatively simple material model.

REFERENCES

1. MacCracken, R., Joy, K.I.: Free-Form Deformations With Lattices of Arbitrary Topology. Proceedings of the 23rd Annual Conference on Computer Graphics and Interactive Techniques 1996: 181–188.
2. Sitek, A., Klein, G.J., Gullberg, G.T., Huesman, R.H.: Deformable Model of the Heart with Fiber Structure. IEEE Transactions on Nuclear Science 2002;49(3):789–793.

210. DEMONSTRATION OF THE BOLD EFFECT IN THE MYOCARDIUM OF THE RAPIDLY BEATING MOUSE HEART IN-VIVO AT 9.4T

Ravi T. Seethamraju, PhD.,¹ George Dai, PhD.,² Matthias Nahrendorf, MD,³ David Sosnovik, MD.⁴ ¹Siemens Medical Solutions, Charlestown, MA, USA, ²Martinos Center for Biomedical Imaging, Charlestown, MA, USA, ³Massachusetts General Hospital and Harvard Medical School, Charlestown, MA, USA, ⁴Martinos Center for

Biomedical Imaging, Massachusetts General Hospital and Harvard Medical School, Charlestown, MA, USA.

Background : Transgenic mouse models plays a central role in the investigation of cardiovascular disease. BOLD imaging has been used in humans and large animal models to probe the vascular function of the coronary circulation and microcirculation. While susceptibility imaging of exogenous iron-oxides has been performed in the hearts of mice in-vivo, to the best of our knowledge, the feasibility of BOLD imaging has not yet been demonstrated. The aim of the study was to extend the phenotypic capabilities of cardiac MRI in mice by demonstrating a flow dependent BOLD effect in the myocardium of a beating mouse heart in-vivo.

Methods: C57Bl/6 mice ($n = 3$) were imaged on a 9.4 T horizontal bore scanner with both ECG and respiratory gating. Body temperature was maintained with a warm air blower. Spoiled T2* weighted FLASH images were obtained with an echo time of 10 ms in the short axis of the heart at the mid-ventricular level. Six images, equally spaced across the cardiac cycle, were acquired after each appropriate physiological trigger. The echo time in each of these images was 10 ms. Other parameters included: FOV 30 mm, slice 1 mm, 200×200 matrix, 30 degree flip angle, 4 signal averages. Two sets of images, exploiting the known vasodilatory properties of isoflurane in the heart, were acquired. An initial set of images was acquired under high flow conditions using a high dose of inhaled isoflurane (2–2.5%), while the second set was obtained under low flow conditions using a lower dose of inhaled isoflurane (1–1.5%). The respiratory gating window was lengthened during the higher dose of isoflurane to account for the slower respiratory rate under these conditions. All other pulse sequence and physiological parameters were left completely unchanged. The images were saved as absolute 16 bit grayscale and Dicom format for offline analysis using the Matlab and Osirix image processing environments. Images were co-registered using rigid registration based on a cross-correlation of the two images. Difference images, with and without image co-registration, were created between identical frames in the two data-sets to detect changes in signal intensity. Particular attention was paid to the signal intensity in the septal, anterior and lateral walls of the left ventricle which, unlike the inferior wall, are not affected by susceptibility artifacts from the lung interface.

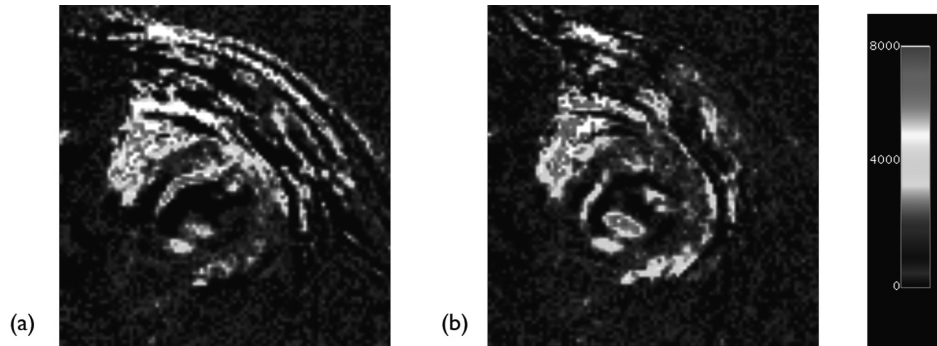


FIG. 1. Difference maps of signal intensity in the mouse heart in-vivo under high and low flow conditions. The increase in myocardial signal intensity seen under high flow conditions is consistent with a BOLD effect. The difference maps have been constructed either without (a) or with (b) prior image co-registration.

Results: All three mice tested, were able to complete the protocol. The duration of the scans obtained under different doses of isoflurane varied by <10% and was approximately 10–12 minutes long in each case. Signal intensity in the left ventricular myocardium was significantly higher under conditions of high flow than low flow, consistent with a BOLD induced signal change (Fig. 1).

This phenomenon was seen both at end diastole (8602 ± 2024 versus 6675 ± 2243) and at midsystole (8694 ± 1944 versus 7040 ± 1841) with $p < 0.05$ by paired t-tests at both time points. Difference maps of myocardial signal intensity readily showed these signal differences particularly when rigid co-registration of the two images was performed prior to subtraction (Fig.1).

Conclusion: The results demonstrate that changes in flow in the myocardial microcirculation can be imaged in the mouse in-vivo with BOLD imaging. With extensive further validation, the possibility of imaging endothelial function and other critical aspects of coronary vascular biology serially and non-destructively in the mouse in-vivo is feasible.

Imaging Research

211. CARDIAC SARCOIDOSIS: A CASE STUDY

Caron Murray, MRT (R), AC(R), MRT (MR). *Sunnybrook Health Sciences Centre Toronto, Ontario, Canada.*

Introduction: Sarcoidosis is a systemic granulomatous disease of unknown etiology that most commonly affects young adults. The identification of cardiac involvement in patients with sarcoidosis is problematic, and the true incidence is unknown. Cardiac magnetic resonance imaging may help quantify the actual incidence of cardiac involvement and may lead to advances in the monitoring and treatment of this disease.

Purpose: To describe a case of cardiac sarcoidosis in a 48-year-old female patient who underwent a Cardiac MR study with delayed enhancement. We report the case of a patient with sarcoidosis in whom cardiac magnetic resonance imaging pro-

vided supportive evidence of cardiac involvement by delineating regions of myocardial involvement inconsistent with ischemic injury.

Methods: A 48-year-old female patient presented to the MR department with a differential diagnosis of query coronary artery disease. MR imaging was performed on a 1.5T CVi MR system (GE Healthcare, Waukesha, USA) using a dedicated cardiac phased-array coil and VCG gating. Standard cardiac images were obtained in diastole to minimize artifact due to cardiac motion. The study consisted of multislice-multiphase steady state-free precession (SSFP) sequences in the short-axis(SA), vertical long-axis (VLA) and 4CH views to assess regional wall motion abnormalities. IR-GRE Perfusion breath-hold imaging was performed in the SA during gadolinium injection. Delayed enhancement SA imaging was performed 10 minutes post

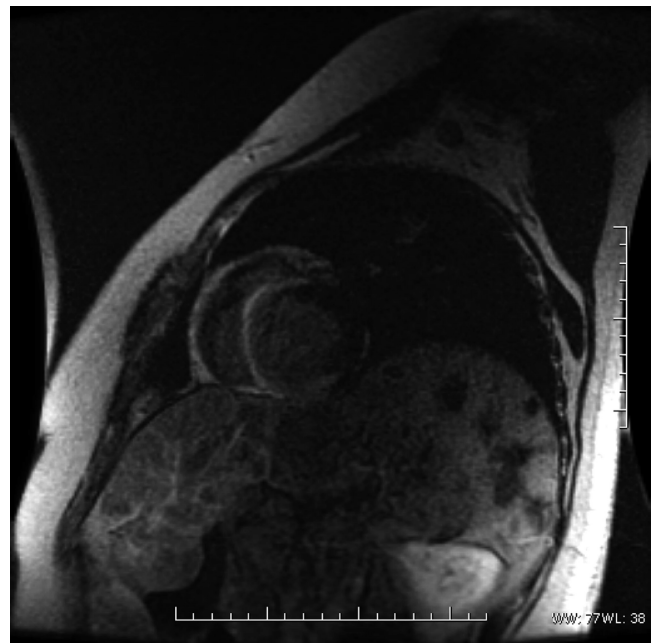


FIG. 1. Delayed enhancement image demonstrating diffuse area of signal hyperintensity.



FIG. 2. SSFP image demonstrating areas of dyskinesia and akinesis.

contrast injection. Additional VLA and 4CH images were acquired with an IR-GRE sequence to assess for the presence of late gadolinium-enhancing lesions.

Results: In our patient, perfusion imaging demonstrated minor persistent perfusion defects inferiorly. However, delayed enhancement imaging showed significant abnormal hyperenhancement in the basal left ventricle involving the septum and inferior walls. Heterogeneous enhancement of these areas with hyperintense signal on the epicardial border of the septum was well demonstrated on the 4 chamber views and short axis views. The septum demonstrated dyskinesia while the inferior wall was akinetic. These patterns of hyperenhancement were inconsistent with ischemic myocardial injury but indicative sarcoid infiltration.

Conclusions: Cardiac MR imaging is a useful noninvasive method for the noninvasive diagnosis and follow-up of cardiac sarcoidosis.

212. USING CMR TO DETECT EARLY CHANGES IN BIOMARKERS OF CARDIOTOXICITY AFTER INITIATION OF CHEMOTHERAPY: FIRST IMPRESSIONS

G Smith,¹ P Kotwinski,² P Gatehouse,¹ J Lyne,¹ M Mutch,² H Montgomery,² DJ Pennell.¹ ¹CMR Unit, Royal Brompton Hospital, London, UK, ²University College London Hospitals, London, UK.

Introduction: Anthracyclines are frequently utilised for adjuvant chemotherapy in patients with breast cancer and many childhood malignancies. This therapy is often cardiotoxic and may lead to impairment of ventricular function and heart failure. The population risk rises with dosage, but the risk to the individual is yet

unknown. This means that patients may be receiving less than optimal dosage due to this possible risk. If we could identify patients at risk, using early markers of cardiotoxicity, we could tailor the treatment for individual patients for optimal effect.

Cardiovascular magnetic resonance (CMR) offers the most accurate and reproducible technique for assessing parameters of cardiac systolic function. This allows maximum statistical sensitivity for detecting real changes in parameters with minimum sample sizes.

Systolic dysfunction occurs at an advanced stage of myocardial disease. It would therefore be desirable to identify markers of myocardial dysfunction that occur early in the disease process. Using myocardial tagging and with the recent availability of retrospective gating for CMR allowing better temporal resolution, diastolic abnormalities may be identified using CMR. Intrinsic myocardial tissue contrast using T2 weighted spin echo and extrinsic late gadolinium enhancement imaging and indices of microvascular function may also be assessed using CMR.

Purpose: This study attempts to identify early markers of anthracycline mediated toxicity which may predict later cardiac dysfunction and thus optimise individual therapy.

Methods: As part of a prospective gene environment study, 276 patients in total are to be scanned before onset and one year after the final cycle of therapy to evaluate changes in cardiac function. Of these, 100 will have an additional examination on the third day after the initial cycle to try to identify changes which may predict cardiac dysfunction. To avoid confounders the study group is designed to be as homogeneous as possible. We will select female Caucasian patients with histologically proven adenocarcinoma of the breast not requiring left sided external beam radiotherapy and with no previous history of cardiovascular disease or chemotherapy. Patients are being recruited via the National Cancer Research Network.

Using a 1.5 T Siemens Avento scanner all patients (105 to date) will undergo CMR to evaluate bi-ventricular systolic and diastolic function using a retrospectively gated high temporal resolution SSFP cine. In addition they will also undergo T2 weighted STIR imaging to detect possible oedema post treatment, myocardial tagging to define contractile and relaxation parameters and a T2* sequence which may define structural changes within the myocardium secondary to chemo-toxicity.

We will also use rapid first pass tracer imaging to detect any hyperaemic changes using a parallel imaging perfusion sequence. After Gd-DTPA bolus injection, relative enhancement of myocardial versus skeletal muscle will be measured for 5 minutes. To identify any previous myocardial damage we will look for late enhancement using an inversion recovery sequence.

The patients are selected consecutively for a repeat scan on day three according to their availability and general wellbeing. Thus far, 43 have returned the day three scan. The protocol is repeated with the exclusion of the late enhancement imaging.

All patients are expected to attend for the one year post last dose of chemotherapy. So far three patients have had the one year follow-up.

Systolic and diastolic functional parameters will be measured using a three dimensional ventricular surface and valve plane reconstruction. Indices of hyperaemia will be assessed using a model based technique with Fermi deconvolution. The cardiac T2* will be compared using dedicated software to investigate any possible myocardial structural change.

213. THE UTILISATION OF NEW CMR TECHNIQUES WITH A PEDIATRIC POPULATION: CASE STUDIES FROM THE ROYAL CHILDREN'S HOSPITAL, MELBOURNE

Glenn Cahoon MAppSc,¹ Michael Ditchfield FRANZCR,¹ Michael Cheung MD,² Michael Kean,¹ Wellesley Were.³

Cardiac magnetic resonance (CMR) represents an ideal technology for the diagnosis and management of pediatric cardiac conditions. Advantages include the ability to image in any plane, accurately quantify blood flow, and conduct functional imaging, without the use of ionizing radiation. These advantages are particularly helpful in delineating the complex congenital abnormalities often found in pediatric conditions. There exist, however, a number of technical challenges with standard CMR techniques that result from smaller anatomical structures, faster heart rates, and poor patient compliance. Recent advances in MRI hardware and sequence design allow us to overcome many of these limitations of spatial and temporal resolution traditionally inherent in pediatric CMR, while dramatically reducing overall scan time. These new advances offer exciting opportunities to greatly increase the utility of CMR with pediatric patient populations.

This presentation is a review of our experience in using these new technologies in pediatric CMR at both 1.5T and 3T over

the past year. The author will describe and present a series of case studies, demonstrating the use of new CMR techniques. These techniques include recent 'works in progress', such as T2 prepared TrueFISP imaging, 3D whole heart morphological studies, time resolved contrast enhanced MRA, phase contrast flow quantification with iPAT (GRAPPA), and dynamic cardiac imaging with TSENSE. This presentation will also describe the fundamentals of CMR pulse sequences, and the integration of these new techniques into our current protocols. In addition, differences in imaging strategies and patient preparation for pediatric CMR will be discussed. The cases, selected from patients referred for CMR at the Royal Children's Hospital, Melbourne, represent a mix of congenital and acquired cardiovascular diseases over a range of age groups from neonatal to adolescent and early adult presentations. All the images were acquired using either our 32 Channel TIM Avanto 1.5T, or TIM TRIO MRI systems. This presentation demonstrates the utility of new advances in CMR to dramatically improve patient diagnostics across a range of pediatric cardiac conditions.

214. MR ASSESSMENT OF LEFT VENTRICULAR SEPTAL ANEURYSM: A CLINICAL CASE STUDY

S. Eder,¹ A.S. Pednekar, PhD,² R.L. Eisner, PhD,¹ A.R. Bhandiwad, MD.¹ ¹Cardiac MR Imaging, Crawford Long Hospital, Atlanta, GA, USA; ²Philips Medical Systems, Bothell, WA, USA.

A 44-year-old man was referred for a cine and contrast enhanced cardiovascular magnetic resonance (CMR) scan for further evaluation of intracardiac mass reported on echocardiogram.

Cardiac MR was performed on a 1.5T, Philips Intera, using a 5-element phased-array surface coil. Fast gradient echo survey

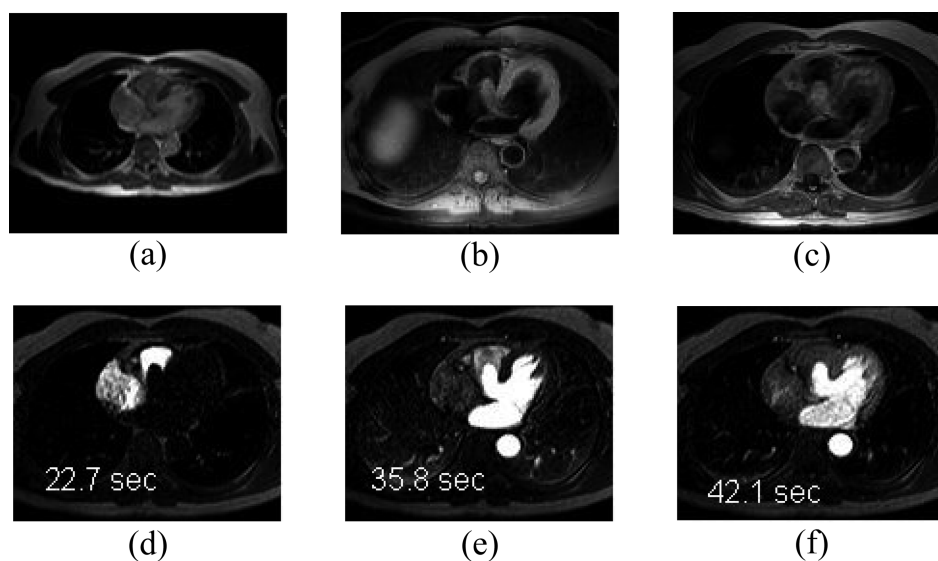


FIG. 1. Axial slice images acquired using (a) Fast gradient echo; (b) T1 weighted dualIR with fat suppression; (c) post contrast T1 weighted dualIR without fat suppression; and perfusion images (d) 22.7sec; (e) 35.8 sec; (f) 42.1 sec after the contrast injection.

images revealed an abnormal structure near the left ventricular outflow tract (LVOT). The T1 and T2 weighted dual inversion recovery black blood (dualIR) images with and without fat suppression were acquired to characterize the tissue of the abnormal structure. The structure was isointense to myocardium on both T1 weighted dualIR images, with and without fat suppression and presented intermediate signal on both T2 weighted dualIR images with and without fat suppression. These images indicated possibility of a very slow blood flow and absence of adipose tissue in the structure. Cine CMR images (steady state free precession sequence) showed that the structure is mobile in coherence with the LVOT and has blood flow in it. Post contrast perfusion (single shot spoiled fast gradient echo sequence with non-slice selective, unshared saturation recovery prepulse) images confirmed the blood flow into the structure during the left ventricular filling phase of the cardiac cycle. No hyper-enhancement was observed on the delayed enhancement (segmented inversion recovery fast gradient echo sequence images) revealing the wall of the structure to be normal. The patient was diagnosed with an aneurysm of the membranous interventricular septum caused by the thinning of the myocardium bulging into the right ventricle. There was no filling defect visualized in the aneurysm, however shunt can not be excluded.

CMR imaging with ability to acquire high-resolution, multi-plane, multi-orientation images allowed to accurately evaluate morphology (location and extent), tissue characteristic, function (mobility), perfusion and viability of the wall of the suspected structure. CMR overcame the limitation of the echocardiography to distinguish the left ventricular septal aneurysm from the suspected intracardiac mass or thrombus.

215. COMBINED EFFECTS OF GADOLINIUM DOSAGE AND DELAY ON MYOCARDIAL NULLING

June A. Yamrozik, RT(R, MR) BS, Janice Meister, Geetha Rayerao, Ronald B. Williams, Diane A. Vido, MS, Vikas Rathi, MD, Mark Doyle, PhD, Robert W.W. Biederman, MD. Department of Cardiovascular Medicine, Center for Cardiovascular MRI, Allegheny General Hospital, Pittsburgh, PA, USA.

Introduction: Optimal nulling in the assessment of myocardial viability using delayed hyperenhancement sequences (DHE) is essential. Numerous strategies have been advocated, but, except for phase sensitive inversion, all require an element of 'guess-work' based on prevailing experience, scanner, and contrast agent. Yet, in the scanning environment, time is of the essence, and selecting the appropriate inversion time (TI) is crucial to capture the passage of contrast wash in/washout curves (e.g., 200ms is not a universal TI). An inappropriate TI with insufficient nulling of the myocardium may markedly impair image quality, with subsequent compromise in the ability to correctly diagnose the patient.

TABLE 1
T1 Relative to Dose/Time

Time/Dose	0.05	0.10	0.15	0.20
5.00	292	252	211	171
10.00	312	272	232	191
15.00	333	292	252	212
20.00	353	313	272	232

Hypothesis: We hypothesize that the dosage of gadolinium and the time post-injection are key determinants of the optimal choice of TI to achieve myocardial nulling for assessment of viability.

Methods: Sixteen patients (8M, 8F), age 21–79 years (mean 54.4 ± 15.7 years) S/P acute myocardial infarction underwent 2 separate cardiac MRI's (CMR), with 2 separate gadolinium doses (Magnevist-Berlex, New Jersey, USA) of 0.1mmol/kg and 0.2mmol/kg within a 2-week period to evaluate myocardial viability using an identical protocol. Scans were acquired on a GE CV/i Excite Version 12, 1.5 T (GE, Milwaukee, WI) system. The sequence utilized for optimum myocardial nulling was 2D Gradient Echo IRP (FGR with inversion recovery prep). An 8-channel or 4-channel cardiac coil was used, dependent on patient size (constant coil configuration for each patient). The sequence parameters were as follows: TE: min, FA: 20, NEX: 2, trigger delay: adjusted to onset of diastole, 1RR interval and TI adjusted to null the myocardium. This sequence was performed at 10 and 20 minutes post-gadolinium.

Results: All patients successfully completed the protocol without complications. Average time for the imaging was 64.4 ± 6 min. No gadolinium side effects were noted. In 16/16 patients (100%), a lower TI was required to null the myocardium with a 0.2 mmol/kg dosage as compared to the 0.1 mmol/kg dose. All but one patient was in normal sinus rhythm; one patient was in controlled atrial fibrillation and had suboptimal nulling. However, a lower TI was still required to null the myocardium using the higher gadolinium dose as compared to the lower dosing strategy. At 10 min post-gadolinium, with the 0.1 mmol/kg dosage the null ranged from 220-335 (mean 268.1 ± 29.0 ms)

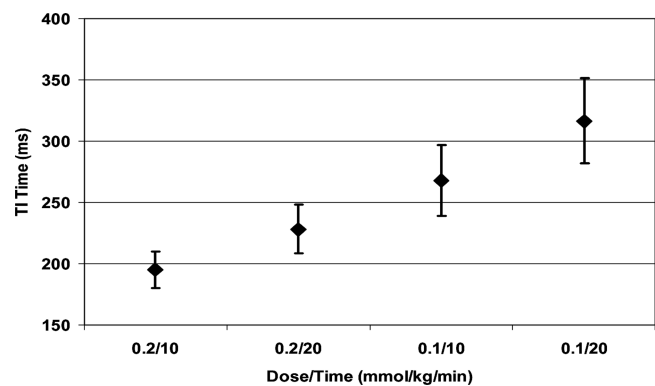


FIG. 1. Linear Response Regression.

and with the 0.2 mmol/kg dosage, the null ranged from 170-225 (mean 195.3 ± 15.2 ms) ($p < 0.001$). At 20 min post-gadolinium with the 0.1 mmol/kg dosage, the null ranged from 245-380 (mean 316.6 ± 34.9 ms) and with the 0.2 mmol/kg dosage the null ranged from 190-260 (mean 228.4 ± 20.1 ms) ($p < 0.001$). (Fig. 1) Multiple linear regression analysis was used to develop a model for predicting nulling TI using time and dosage information. Both time and dosage were found to be significant predictors of nulling, and the two predictor model was able to account for 76% of the variance ($p < 0.01$). The equation is: $TI = 311.6 + (4.1 * Time) - (804.7 * Dosage)$, Table 1.

Conclusion: Optimal nulling of the myocardium in the DHE sequence is required, but searching for this during the time constraints of the scan session can be both tedious and time consuming. The TI Predictor Model can be used to give a more accurate and reliable TI. Our data indicate that whatever dosage of gadolinium and timing strategy is used, a predicted T1 can be used when initiating scanning, avoiding the element of "guesswork". This information follows a predicted and expected T1 decay curve but one that may be overlooked in the common clinical setting, while most helpful to know and apply when variable contrast dosing strategies are available. Convention suggests a TI of 200ms is generally the optimal myocardial null time, however, an awareness of contrast dosage and timing strategy is most essential for more accurately determining this factor.

216. VALVULAR ENHANCEMENT: ARE WE OVERLOOKING SOMETHING?

Ronald B. Williams, Mark Doyle, PhD, June Yamrozik, Ketheswaram Caruppanan, MD, Vikas Rathi, MD, Geetha Rayarao, Diane Vido, Robert W.W. Biederman MD. Department of Cardiac Magnetic Resonance Imaging, Division of Cardiology, Allegheny General Hospital, Pittsburgh, PA, USA.

Introduction: The presence of late gadolinium enhancement (LGE) by CVMRI (CMR) is the reference standard for deter-

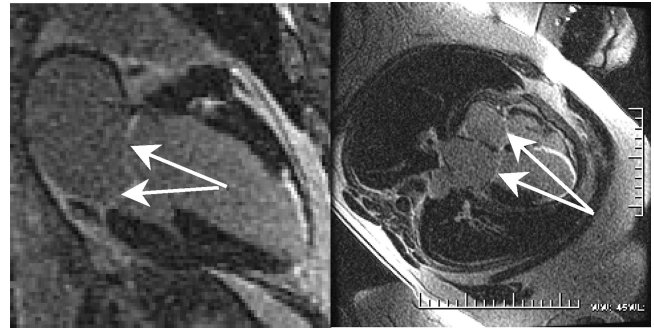


FIG. 1. LGE demonstrating post contrast valvular enhancement.

mining myocardial viability in the post-MI patient. Evaluation by DHE has traditionally been limited to myocardial processes. Yet, we have previously shown that DHE signal may be seen in the post-MI valvular apparatus as well. However, the remodeling implications for the valvular apparatus with DHE signal are not known.

Hypothesis: We hypothesize LGE can be detected in the mitral valvular apparatus in post-MI patients and its presence is predictive of annular remodeling.

Methods: One hundred sixty-four (164) pts; (111) post MI (38 F, 37 acute, 74 chronic) underwent LGE MRI (1.5T GE CV/i, Excite HD, Milwaukee, WI.) with 0.2 mmol/kg Magnevist (Berlex, Wayne, NJ) or 0.1 mmol/kg MultiHance (Bracco, Princeton, NJ). Notation of presence of LGE pattern involving mitral valve (MV) and/or mitral annulus was made. Non-MI patients (53) were used as controls. A subset of the post-MI patients (8) were analyzed for annular diameter changes, measured in three views when available, at baseline and at follow-up, up to one year.

Results: In all post-MI patients, the region of infarction was confirmed by functional analysis and by DHE. In the post-MI group, LGE was observed in the mitral valve in 73% (81/111) while the mitral annulus was enhanced in 40% (45/111) (Fig.1). In addition, it was noted that there was enhancement in the aortic



FIG. 2. Annular dimension locations in 2 Ch, 4 Ch, and 3 Ch views.

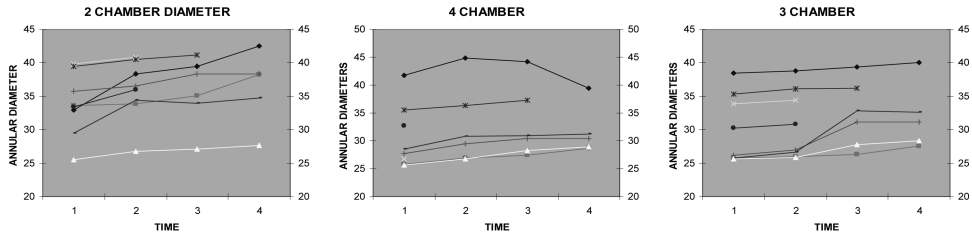


FIG. 3. Serial evolution of mitral annular diameter.

(AV) and tricuspid (TV) valves on occasion (AV: 25/111, 22%; TV: 33/111, 30%), Fig. 1. In the subset of eight patients with serial DHE studies demonstrating valvular enhancement, we measured the mitral annulus diameter for dimensional changes, (Fig. 2). We observed a gradual increase in diameter over time 32.7 ± 5.1 to 34.4 ± 4.9 mm, $p < 0.001$ (Fig. 3).

Conclusion: CMR LGE permits detection of mitral valve and mitral annulus enhancement in post-MI patients. This observation suggests that CMR may detect and as yet an unidentified process (possible an inflammatory component) effecting valvular apparatus in the post-MI patient, and potentially a precursor to mitral valve dysfunction and/or LV remodeling.